CONF-851201--4

Experimental and Analytical Study of Loss-of-Flow Transients in EBR-II Occurring at Decay Power Levels*

CONF-851201--4

DE86 004064

by

L. K. Chang, D. Mohr, E. E. Feldman,
P. R. Betten and H. P. Planchon

Argonne National Laboratory
Argonne, Illinois 60439

To be presented
at the
Conference on Alternative Energy Source
Miami Beach, Florida
December 9-11, 1985

*Work supported by the U. S. Department of Energy, Reactor System, Development and Technology, under Contract W-31-109-Eng-38.

57100 B

Experimental and Analytical Study of Loss-of-Flow Transients in EBR-II Occurring at Decay Power Levels*

L. K. Chang, D. Mohr, E. E. Feldman
P. R. Betten and H. P. Planchon

Argonne National Laboratory
Argonne Illinois 60439

ABSTRACT

A series of eight loss-of-flow (LOF) tests have been conducted in EBR-II to study the transition between forced and natural convective flows following a variety of loss-of-primary-pumping power conditions from decay heat levels. Comparisons of measurements and pretest/posttest predictions were made on a selected test. Good agreements between measurements and predictions was found prior to and just after the flow reaching its minimum, but the agreement is not as good after that point. The temperature are consistent with the flow response and the assumed decay power. The measured results indicate that the flows of driver and the instrumented subassemblies are too much in the analytical model in the natural convective region. Although a parametric study on secondary flow, turbulent-laminar flow transition, heat transfer ability of the intermediate heat exchange at low flow and flow mixing in the primary tank has been performed to determine their effects on the flow, it is still unknown the cause of the discrepancy at very low flow level.

1. INTRODUCTION AND BACKGROUND

The ability of natural convection to remove decay heat from the reactor following a loss-of-coolant-pumping-power event is one of the major concerns in the safety assessment of a reactor. An extensive testing program has been developed using the in-core instrumented subassemblies to study the decay heat removability and dynamic plant response of the Experimental Breeder Reactor II (EBR-II) [1] following a variety of LOF events. Previous testing programs utilized two instrumented subassemblies, XX07 [2] and XX08 [3], they were installed in the EBR-II to investigate natural convective behavior of the re-

*Work supported by the U. S. Department of Energy, Reactor System, Development and Technology, under Contract W-31-109-Eng-38.

actor under a variety of loss-of-flow (LOF) conditions during the 1970's. The most severe experiment in the XX07 test series was identified as Test F, which was a delayed LOF test conducted shortly after reactor shutdown from rated power when the primary pumps had already been shut down. Test F was initiated by tripping the primary auxiliary pump. Because the sodium outlet temperature (SOT) thermocouples indicated that the maximum acceptable temperature was exceeded during the test, Test F was prematurely terminated; however, the peak in-core temperatures had already been reached. In the XX08 test series, LOF tests initiated from both fission and decay power levels were conducted with various degrees of buoyancy driving forces imposed external to the core. This was accomplished by varying the primary and secondary pump coastdown speed and the auxiliary pump operating conditions.

The purpose of the present EBR-II Shutdown-Heat-Removal Test (SHRT) program is to further use the EBR-II plant to investigate natural-convective-cooling phenomena in liquid metal reactors (LMRs) during a variety of protected (with scram) transients and to initiate experimental studies of the inherent shutdown and decay heat removal capability for unprotected (without scram) transients [1,4]. The SHRT program consists of some 50 individual tests, which has been categorized into five types based on test similarity and behavior. The five types are (1) protected LOF from fission power, (2) loss-of-flow from decay power levels, (3) reactivity feedback verification, (4) unprotected LOF, and (5) unprotected loss-of-heat-sink. Types 1 and 2 tests were designed to provide information on natural convection of the reactor following LOF transients initiated from various fission or decay power conditions. The objective of type 3 tests was to characterize the EBR-II reactivity feedback behavior, in which the reactor power and temperature responses were studied by perturbating separately the reactor flow and inlet temperature. The results obtained from these tests were used to validate the neutronic feedback models in the code and to assure safe performance of the unprotected LOF tests [5,6]. Tests of types 1, 2 and 3 were successfully conducted in June of 1984. The purpose of types 4 and 5 is to investigate the inherent shutdown capability of the EBR-II plant following a LOF, a loss-of-heat-sink [7] or a loss-of-steam-pressure event. A portion of the type 4 and 5 tests was completed in May 1985.

Experimental and analytical studies of type 2 tests are the subject of the present investigation. Eight tests were included in the group to experimentally determine decay heat removability of EBR-II under a variety of decay heat levels and primary flow coastdown conditions. This information would not only provide additional understanding and insight relative to operational reactor reliability and safety of EBR-II, but could also be applicable to the design and performance assessment of other LMR designs. Furthermore, data obtained from the tests could be used to validate the general purpose thermal-hydraulic system analysis codes used in the design and safety evaluation of LMR plants.

Instrumented subassemblies (INSATs) XX09 and XX10 [8] were used to provide temperature and flow measurements for the tests. Design basis and verification of temperature predictions of INSATs XX09 and XX10 were discussed in refs. [9,10].

The thermal-hydraulic-neutronic system code NATDEMO [11] was used to predict the plant response of the tests, while our hot channel analysis code HOTCHAN was employed to determine the thermal-hydraulic response of the individual subassemblies, particularly the XX09 and hottest drivers. The measurements of selected tests were compared with pretest and posttest predictions. In this paper, the effects of decay power levels and primary coastdown rate on the reactor temperature response were investigated.

II. EBR-II REACTOR PLANT AND INSTRUMENTATION

The EBR-II is a sodium-cooled, pool-type fast reactor, which currently operates at a thermal power level of 60 MW and a net electrical power output of about 20 MW. Rated flow rates of the reactor and secondary systems are 464 and 284 kg/s, respectively. The plant is located in Idaho and is operated by Argonne National laboratory for the U. S. Department of Energy. EBR-II has been in operation since 1964 and has served primarily as a fast-flux irradiation facility since 1967. Recently it is also served as a reactor safety testing facility.

A schematic representation of the EBR-II plant is given in Fig. 1. Since the reactor is basically of the pool design, essentially all primary components are submerged in a large volume of sodium within the primary tank. Primary coolant is well-mixed in the common outlet plenum which is connected to the outlet "Z-pipe" that transports the coolant about 12 m to the IHX.

Flow exits from the IHX through a continuous radial gap near the bottom, where it mixes with the bulk sodium in the primary tank before it enters the two primary pumps and about 10 m of reactor inlet piping. The IHX transfers the energy generated in the reactor to the secondary sodium system and ultimately to the steam generators and turbogenerator. During the tests, however, the steam is normally bypassed around the turbine directly to the condenser. The secondary sodium returns to the IHX after passing through the superheaters, evaporators and about 240 m of piping.

The EBR-II plant is well-instrumented throughout the core and the balance of plant. The instrumentation in the primary system includes flowmeters, bulk-sodium thermocouples, and reactor sodium inlet and outlet thermocouples. The primary system flowmeters are located near both the inlet and the outlet of the reactor. The bulk-sodium thermocouples are at various axial and circumferential locations in the primary tank and the thermocouples measuring the sodium outlet temperature (SOT) from the core are 6.35 mm above the subassembly outlet and are distributed over the 16 rows of subassemblies. Measurements of coolant temperature in the reactor outlet plenum were made by the upper-plenum instrument probe. The probe is above the outer blanket region and has thermocouples at eight axial positions in the outlet plenum. The fisssion power of the reactor is measured by an ion chamber and is also calculated by heat balances based on temperature and flow measurements of the primary, secondary and steam systems. The excess reactivity is evaluated based on power measured from ion chamber signal with an inverse kinetics routine. Both measured data and internally calculated data are recorded on magnetic tape by the data acquisition system (DAS). The secondary sodium and steam systems are also well-instrumented with thermocouples, pressure transducer and flowmeters.

The instrumented subassemblies (INSATs XX09 and XX10) are being used to measure in-core coolant temperatures and flows; the analytical predictions can thus be verified by measurement. The XX09 INSAT, as shown in Fig. 2, is a 61 element Mark-II driver-fuel type subassembly. Fifty-nine of the 61 positions are occupied by standard Mark-II fuel elements containing a tag gas, and the remaining two positions are hollow tubes used as conduits for passage of the flowmeter flow and thermocouple leads through the core. The elements have been placed in a standard control rod hexagonal can made of 316 stainless steel. XX09 is inserted in row 5 of the core and is compatible with control rod number 2 location, and has a total of 28 thermocouples which are used to monitor coolant temperatures within the subassembly. There are two thermocouples located in the flowmeter near the inlet, five thermocouples at the core midplane, thirteen thermocouples placed 0.021 m below the top of the fuel, four thermocouples placed 0.137 m above the core, two thermocouples near the subassembly outlet, and two thermocouples in the annular bypass region near the outlet. The two flowmeters in XX09 are located in tandem in the lower shield section below the fuel element T-bar grid. The INSAT XX10 is a 19-element non-fueled instrumented subassembly, which is a simulated blanket subassembly whose design was based on thermal-hydraulic nondimensional scaling analysis of the blanket subassemblies of two large protypical LMRs. XX10 has a total of 26 thermocouples and two flowmeters to measure the sodium temperature and flow.

III. TEST DESCRIPTIONS

Eight natural convective tests, referred to as SHRTs 2, 3, 8, 10, 12, 14, 16 and 18 in the SHRT program, were conducted from shutdown conditions. Thus, the reactor was subcritical and the only power was from fission-product decay. Most of the tests (SHRT's 3-18 in Table I) were initiated by tripping the primary main coolant pumps and the auxiliary pump after running the primary coolant pumps at high flow for about 10 minutes after reactor shutdown to attain a near isothermal condition prior to the test transients. These tests were initiated about one hour after reactor shutdown from either rated or 75% of rated power. SHRT 2 is the most unique test in this group and is a repeat of Test F of the XX07 test series conducted in 1974. The test was conducted 20 minutes after the reactor shutdown from rated power, and the transient was initiated by tripping the auxiliary after the main primary pumps had already been deenergized. The auxiliary pump provides about 5% of the rated flow when the main pumps are not in operation. SHRT 2 is the most severe test in the group because of the high decay power and rapid flow coastdown of the auxiliary pump.

A brief description of tests in this series is given in Table I, which summarizes initial conditions of the tests. There are two modes of primary trips employed in this test series. In mode 1 the test was initiated by simultaneously tripping motor-generator and clutch breakers of the primary pumps, and in mode 2 the test was initiated by tripping clutch breakers only.

TABLE I. Test Description

SHRT No.	Initial Decay Power Conditions	Initial Primary Flow, % of rated	Initial Secondary Flow, % of rated	Reactor Inlet Temperature, °C	Test Description
2	Test was initiated 20 minutes after reactor shutdown from rated power	~ 5	2	371	Test was initited by tripping the auxiliary pump. The secondary flow was held to its initial value
3	Test was initiated one hour after reactor shutdown from rated power	100	9	371	Test was initiated by tripping the primary pumps (mode 2). The secondary flow was held to its initial value
8	Test was initiated one hour after reactor shutdown from 75% of rated power	100	10	366	Test was initiated by tripping the primary pumps (mode 1). The secondary flow was held to its initial value
10	Same as above	100	0.5	366	Same as SHRT 8
12	Same as SHRT 3	100	0.5	366	Same as SHRT 8
14	Same as SHRT 8	100	10	357	Test was initiated by simultaneously tripping the primary (mode 1) and the secondary pumps
16	Same as SHRT 8	75	10	345	Test was initiated by tripping the primary pumps (mode 1). Fifteen minutes after the transient, the secondary flow was reduced to 5% at a rate of 0.5%/s
18	Same as SHRT 3	100	0.5	352	Test was initiated by tripping the primary pumps (mode 1). Fifteen minutes after the transient, the secondary flow was increased to 10% at 0.5%/s

The approximate primary pump coastdown times from rated flow conditions are 55 and 26 s for modes 1 and 2, respectively. The auxiliary and secondary pumps are the electromagnetic type and contain essentially no stored energy, the flow coastdown characteristic is therefore rapid and depends upon the initial kinetic energy of the fluid and its dissipation rate during the coastdown.

4. ANALYTICAL APPROACH

The NATDEMO and HOTCHAN computer codes were used for temperature predictions of the tests. NATDEMO is a thermal-hydraulic-neutronic system analysis code, which was specifically designed to model the EBR-II plant as shown in Fig. 1, from the reactor to the steam generating system. Detailed descriptions of the NATDEMO code has been given in ref. [11]. The code models the 16 rows of subassemblies by dividing these into three regions; the driver fuel core, the stainless steel reflector, and the depleted uranium blanket regions. Each of these regions has a separate power generation model containing both prompt and delayed components. Fission power was derived from a point kinetics model with six neutron groups. All three regions are described by similar thermal-hydraulic models which treat these as parallel channels operating with individual flow and buoyancy characteristics and a common pressure drop. The reactor power during the tests results from fission product energy release after shutdown, and it has a significant effect on predicted reactor temperatures. The decay power was estimated based on semi-empirical data derived by Shure [12,13] for decay power release after thermal-neutron-induced fissioning of ^{235}U during power operation. Although there might be some differences between the fission product contributions in fast and thermal reactor [14], large differences are neither expected nor have been found to date.

NATDEMO calculates dynamic information on the thermal-hydraulic environment for driver region. The information is used in HOTCHAN as boundary conditions to describe the temperature environment for a single subassembly. HOTCHAN calculates temperatures of a single subassembly. It is an axisymmetric thermal-hydraulic model, and uses transient thermal boundary conditions to calculate intersubassembly heat transfer between the center subassembly and the adjacent six subassemblies. HOTCHAN is capable of predicting the temperature of either a 91-pin or a 61-pin subassembly with driver fuel including the bypass flow region of the latter. The 91-pin driver subassembly was radially divided into three regions to represent the fuel bundle; while in the case of a 61-pin subassembly with bypass flow (i.e., XX09), two regions were modeled to represent the fuel elements and one region to represent the bypass flow region.

The SHRT tests were designed to limit the fuel-cladding temperature to the eutectic temperatures of the fuel elements. These temperatures are 715 and 705°C for the EBR-II driver and blanket fuel elements, respectively. The hottest subassemblies were identified and pretest predictions of the thermal-hydraulic responses of the EBR-II plant and individual subassemblies (basically XX09 and the hottest driver) were determined to assure safe performance of the test and the subassembly temperatures remained within the specified limits

V. EXPERIMENTAL RESULTS

Most of the tests in this series (SHRTs 3-18 in Table I) were conducted about one hour after reactor shutdown. Instrumentation to measure decay power directly is not available in EBR-II and the decay power was calculated to be ~ 1% of the prior operating power after a shutdown time of one hour. In SHRT 2 the test was performed only 20 minutes after reactor shutdown and the initial decay power was estimated to be 1.6% of the rated power. The experimental data recorded on magnetic tape were processed and the instrumentation offsets (error) of the primary system were corrected from measurements at full flow and zero fission power conditions (isothermal). These offsets were then incorporated into the raw data to obtain the final corrected experimental results.

In all of the tests the reactor temperature increases drastically as flow decreases, and the in-core temperatures reach a maximum while the flow is approaching a minimum value. The rising core temperatures increase the thermally induced buoyancy in the primary circuit and then cause the flow to increase somewhat. The effect of the increasing flow and slowly decreasing decay power result in the coolant temperatures to decrease after the maximum transient temperatures have been reached. The peak temperatures of all tests are tabulated in Table II at various axial locations. Sodium temperatures of both the inner and outer regions are given at the TTC location. The former was the average temperature of TTCs 15, 29, 30, 31, 32 and 47, while the

TABLE II. Temperature Measurements of INSATs XX09

SHRT No.	Reactor Inlet Temperatures, °C (°F)	Peak Temperatures at TTC Location, °C (°F) Inner Region	Outer Region	Peak Temperatures at 14TC Location °C (°F)	Peak Temperatures at Subassembly Outlet, °C (°F)
2	371 (700)	520 (969)	511 (953)	494 (921)	480 (897)
3	371 (700)	497 (926)	491 (916)	480 (897)	446 (836)
8	366 (690)	438 (820)	441 (825)	432 (809)	415 (765)
10	370 (698)	470 (878)	464 (868)	454 (849)	432 (809)
12	367 (692)	483 (902)	477 (892)	466 (870)	438 (820)
14	351 (665)	433 (812)	430 (806)	422 (792)	400 (752)
16	349 (660)	448 (838)	443 (830)	438 (820)	415 (780)
18	355 (671)	477 (892)	472 (881)	463 (865)	435 (814)

latter was obtained by averaging TTCs 8, 27, 28, 33, 34, 35 and 53 (see Fig. 2). Due to the initial high flow and low decay power levels, the initial steady-state temperature rise of most of the tests (SHRTs 3-18) is negligible (about 1°C). The average temperature rise of INSAT XX09 for SHRT 2, however, during initial steady state condition is about 37°C. The results in Table II indicate that the transient temperature rise is mild for all the tests, and the natural convective flow is more than adequate to remove the decay heat without overheating the hottest subassemblies.

SHRT 2 is the most severe test in this series and the relatively high temperature is caused by high decay power and rapid pump coastdown following the auxiliary pump trip. The primary natural convective flow is somewhat governed by the secondary flow, and the effect of secondary loop conditions on natural convection of the primary flow is illustrated in SHRTs 8 and 10. These two tests are similar except that in SHRT 8 the initial secondary flow is 10% and in SHRT 10 in the secondary flow is 0.5% of the rated value. The lower temperature in SHRT 8 is caused by more convective flow in the primary loop resulting from higher secondary flow. The effects of primary pump coastdown speed and secondary flow on core temperatures can be demonstrated by comparing SHRTs 3 and 18. Initial power of both tests is similar, and the higher peak temperature in SHRT 3 is due to higher reactor inlet temperature. The faster pump coastdown (26 sec. vs 55 sec.) in SHRT 3 is offset by its higher secondary flow. Two pairs of tests, namely SHRTs 12 and 18, and SHRTs 8 and 14, were designed to demonstrate test repeatability at different decay power levels. The slight discrepancy in temperature measurement is probably caused by the difference of initial decay power because it is a functin of power history and also the primary pump coastdown characteristic since slight variation from test to test is possible.

VI. COMPARISON OF MEASUREMENTS WITH ANALYTICAL PREDICTIONS

In all of the tests, there is generally good agreement between pretest predictions and measured XX09 temperatures up to and including the peak values, and the temperatures were under predicted after the peak. The XX09 flowmeters indicated that the flow are somewhat smaller than the analytical prediction in the natural convective region, and that flow resistance of XX09 is thus larger than expected.

Because SHRT 2 is the most severe test in the series and also has unique initial conditions, this test was selected in this paper to demonstrate a detailed comparison of the experimental data with pretest and posttest predictions. SHRT 2 was conducted 20 minutes after the reactor had been shut down from rated power operation and the test was initiated by tripping the auxiliary pump after the primary main pumps had been already turned off well prior to the test.

In the pretest prediction, the initial decay power of the drivers was based on the expected reactor power history for the test; it was estimated to be 1.8% of the rated power at the test initiation. After the primary main pumps were turned off and steady-state conditions were established, the auxiliary flow was assumed to provide 5.5% of the rated flow; this value was based on the average measured data of several flowmeters in the primary circuit. The secondary flow of 2% with an IHX secondary flow inlet temperature of 304°C were used in the pretest predictions. The flow vs. pressure correlation of the XX09 INSAT used in the analysis was obtained based on XX09 hydraulic tests in the water loop with both laminar and turbulent regions included. At rated conditions, the XX09 power and flow were assumed to be 469 kW and 2.71 kg/s. These values are slightly higher than test data presented in ref. 9. Comparisons of measured and predicted flows of average driver and the XX09 are given in Figs. 3 and 4*, respectively. Both figures indicate that initial auxiliary pump flow assumed in the pretest predictions was considerably higher than the measurements. Generally there is good agreements, however, between experimental data and pretest prediction prior to the time of minimum flow (i.e., force flow period), and the agreement is not so good afterward (natural convective region). The discrepancies are probably caused by (1) difference of initial primary flow rates, (2) differences of secondary flow rates and heat transfer performance of IHX at very low flow, and (3) differences of the hydraulic characteristics of XX09 and drivers in the laminar flow region. Measured and predicted XX09 temperatures at the TTC location are compared in Figs. 5 and 6 for inner and outer regions, respectively, and the average XX09 sodium temperature responses at 14TC position is given in Fig. 7. The results show that there is good agreement between

*The upper flowmeter measured higher flow than that of the lower flowmeter in the low flow region. Average values were used in the figure.

measurements and predictions at and prior to the temperatures reaching their peaks, but the discrepancies increase with time after the peaks. This phenomenon is consistent with the discrepancies in XX09 flow measurements and pretest predictions. The measured XX09 sodium temperature at the subassembly outlet, as shown in Fig. 8 was obtained by averaging two thermocouple readings near the outlet location; here there is good agreement between the experimental data and the pretest predictions.

The decay power can only obtained indirectly by using the measurements of flow and temperature that are available. In the posttest analysis, the initial primary flow inputs of the reactor and XX09 were obtained based on measurements, and the decay power was adjusted to match the initial temperature rise. Parametric study was performed in the posttest analysis in an attempt to match the measured and the predicted flow. The flow mixing in the primary tank and heat transfer performance of IHX at low flow were studied, and the their effects on calculated flow and temperature behavior are small when these parameter were adjusted within reasonable range. The XX09 flow-pressure drop characteristic was also investigated. In the pretest prediction, the transition from turbulent flow to laminar flow was assumed to occur at 1.3% of rated flow. This flow transition value (WTL) has significant effect on the XX09 flow and its effect is demonstrated in Fig. 9, in which the secondary flow remains at 2% of the rated value (WS) throughout the transient. The variation of WTL only results a shift in flow and the flow transient shape only changes slightly in the low flow region. The effects of secondary flow rates are illustrated in Fig. 10 with WTL = 0.013 for all calculations. Again, a translation of flow occurs by varying the secondary flow, however, flow transient pattern remains also the same in the natural convective region. In the posttest analysis, WTL = 0.02 and WS = 0.02 were assumed, and a comparison of predicted and measured flow and temperatures are given in Figs. 3 to 8. Although posttest calculatins indicate better agreement between predictions and measurements, discrepancy in the natural convective region still exists. When the measured XX09 flow was used in thermal prediction, the measured and the calculated temperatures agree well in the low flow region.

VII. CONCLUSION

Both experimental and analytical results indicate that the natural convective flow in EBR-II was adequate to remove the decay heat without overheating the reactor core. The experimental data and analytical predictions agree very well up to the time of peak core temperature, and the agreement is not so good after the peak. This phenomenon appeared in all of the tests. The data seem to indicate that in the laminar flow region, the XX09 flow-pressure drop characteristic in the reactor is somewhat different from that obtained from the laboratory test, and it may vary depending on whether the flow is increasing or decreasing. The discrepancy may also be caused by friction loss in modeling of the primary flow, such as friction in the primary pump propeller. A more in-depth investigation is required for code validation.

References

1. R. M. Singer et al., "Decay Heat Removal and Dynamic Plant Testing at EBR-II," Second Specialists' Meeting on Decay Heat Removal and Natural Convection in LMFBR's, Upton New York, April 17-19, 1985.
2. R. M. Singer and J. L. Gillette, "Measurements of Subassembly Core Temperature Distribution in an LMFBR," AIChE Symp. Series 164, 73, Nuclear Solar, and Process Heat Transfer, St. Louis, pp. 97-104, (1976).
3. J. L. Gillette et al., "Experimental Study of the Transition from Forced Natural Convection in EBR-II at Low Power and Flow," Trans. ASME (J. Heat Transfer) 102, pp. 525-530 (1980).
4. H. P. Planchon et al., "The EBR-II Inherent Shutdown Heat Removal Tests - A survey of Test Results," Intl. Topical Meeting on Fast Reactor Safety, Knoxville, Tennessee, April 21-25.
5. L. K. Chang and D. Mohr, "The Effect of Primary Pump Coastdown Characteristics on Unprotected Loss-of-Flow Transients in EBR-II," Second Specialists' Meeting on Decay Heat Removal and Natural Convection in LMFBR's, Upton, New York, April 17-19. 1985.
6. D. Mohr and L. K. Chang, "Perturbation of Reactor Flow and Inlet Temperature in EBR-II for Reactivity Feedback Validation," Intl. Topical Meeting on Fast Reactor Safety, Knoxville, Tennessee, April 21-25.
7. E. E. Feldman and D. Mohr, "Unprotected Loss-of-Heat Simulation in the EBR-II Plant," ASME 84-WA/HT-7.

8. J. Poloncsik et al., "The EBR-II Instrumented Subassemblies, INSAT XX09 and INSAT XX10," Proc. Conf. Fast, Thermal and Fusion Reactor Experiments, Salt Lake City, Utah, April 12-15, 1982.
9. P. R. Betten et al., "Verification of Steady-state Temperature Predictions in an Instrumented LMFBR Driver Subassembly," Third Intl. Meeting on Reactor Thermal Hydraulics, Newport, Rhode Island, October 15-18, 1985.
10. P. R. Betten et al., "Conceptual Design Basis and Temperature Predictions in a Simulated Instrumented LMFBR Blanket Subassembly, "Third Intl. Meeting on Reactor Thermal Hydraulics, Newport, Rhode Island, October 15-18 1985.
11. D. Mohr and E. E. Feldman, "A Dynamic Simulation of the EBR-II Plant During Natural Convection with the NATDEMO Code," Decay Heat Removal and Natural Convection in Fast Breeder Reactors, Hemisphere Publishing Corp. pp. 207-223 (1981).
12. K. Shure, "Fission Product Decay Energy," WAPD-BT-24, Bettis Technical Review 1-17, 1961.
13. K. Shure, "^{235}U Fission Product Decay Energy-1972 Reevaluation," USAEC Report WAPD-TM-1119, Westinghouse Electric Corp., NTIS 1972.
14. B. D. Turland and R. S. Peckover, "The Distribution of Fission Product Decay Heat," UKAEA Culham Laboratory, Oxon, U. K. (1976).

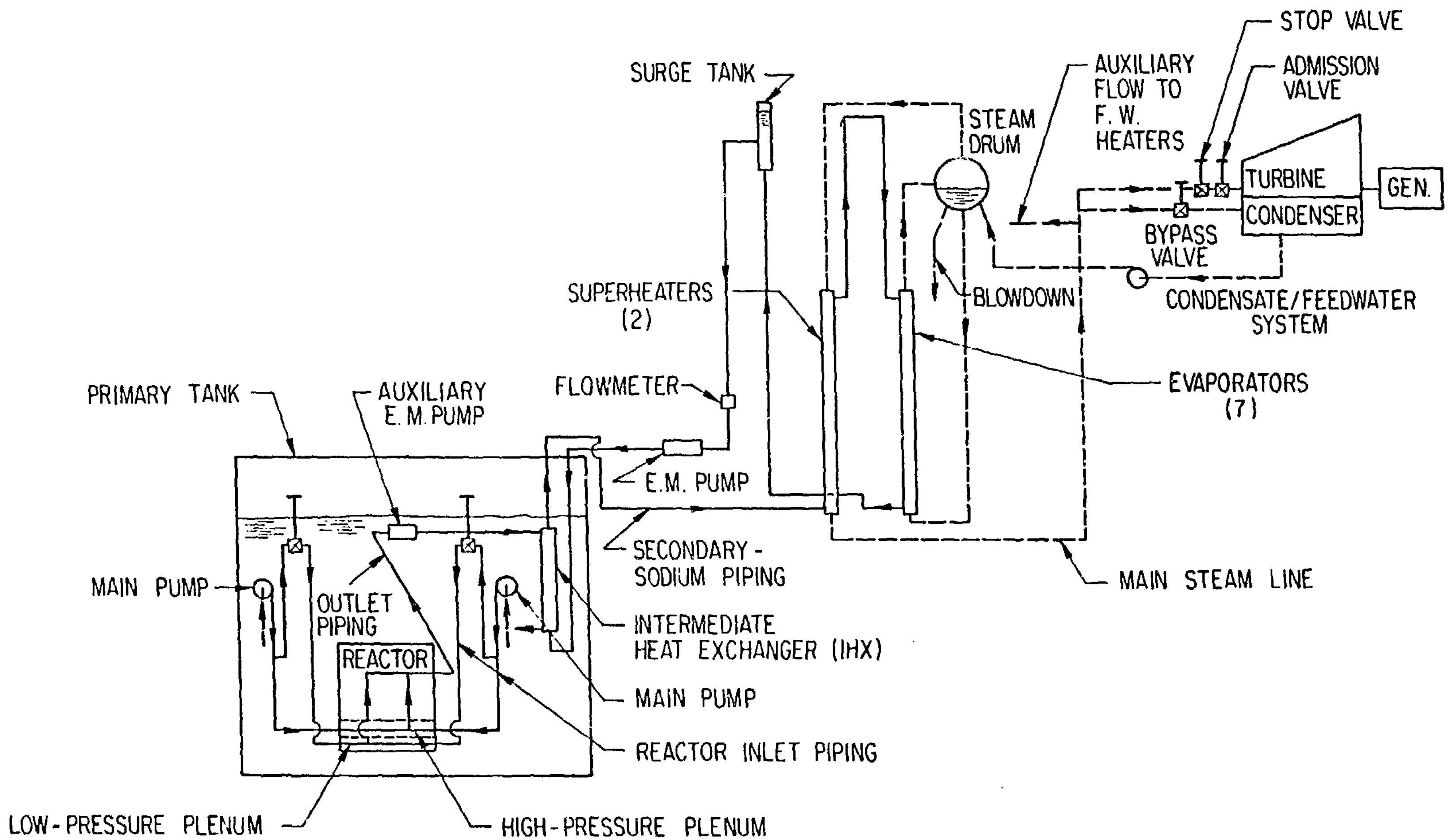

Figure 1. Schematic of EBR-II Plant

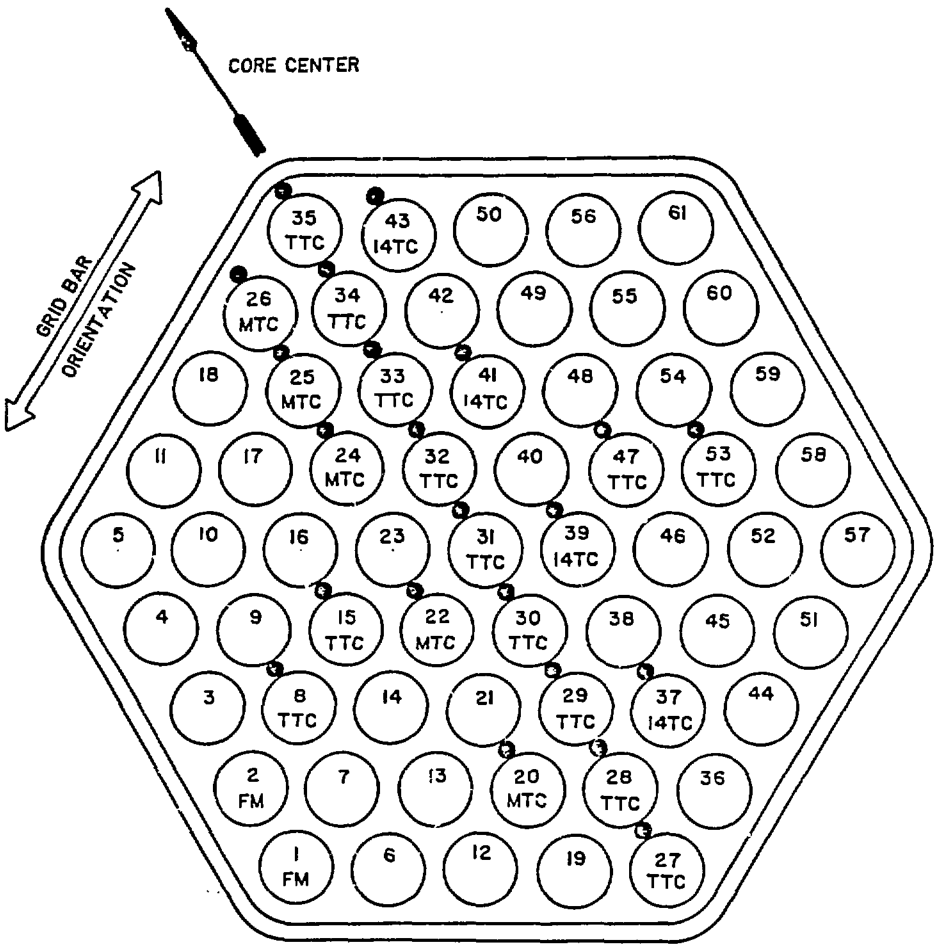

LEGEND

ABOVE CORE TC	14TC	4
MIDPLANE CLAD TC	MTC	5
TOP OF CORE	TTC	13
FLOWMETER CONDUIT LEADS	FMC	2
OUTLET COOLANT TC	OTC	2 (NOT SHOWN)
ANNULUS THIMBLE REGION TC	ATC	2 (NOT SHOWN)
FLOWMETER TC	T	2 (NOT SHOWN)
FLOWMETER	FM	2 (NOT SHOWN)

Figure 2. XX09 Instrumented Subassembly

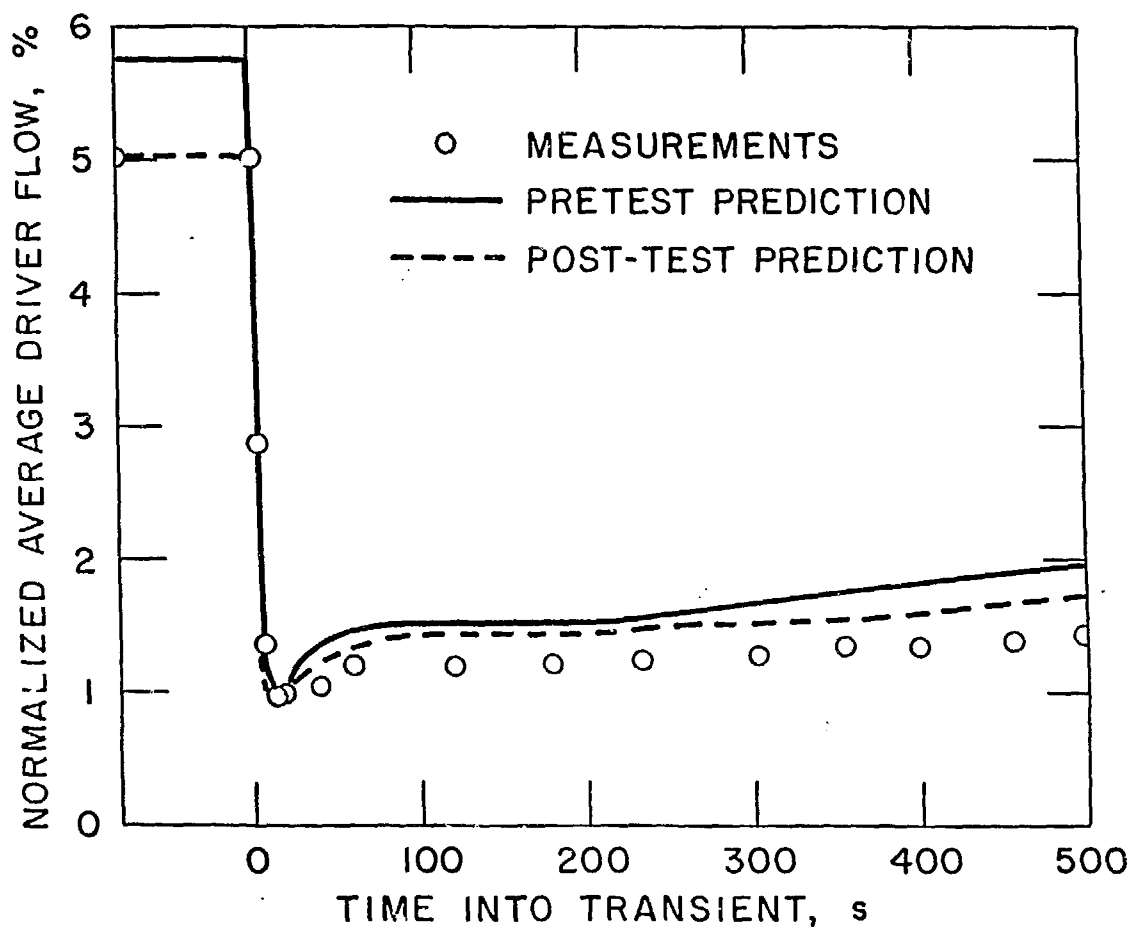

Figure 3. Average Driver Flow During SHRT 2 Transient

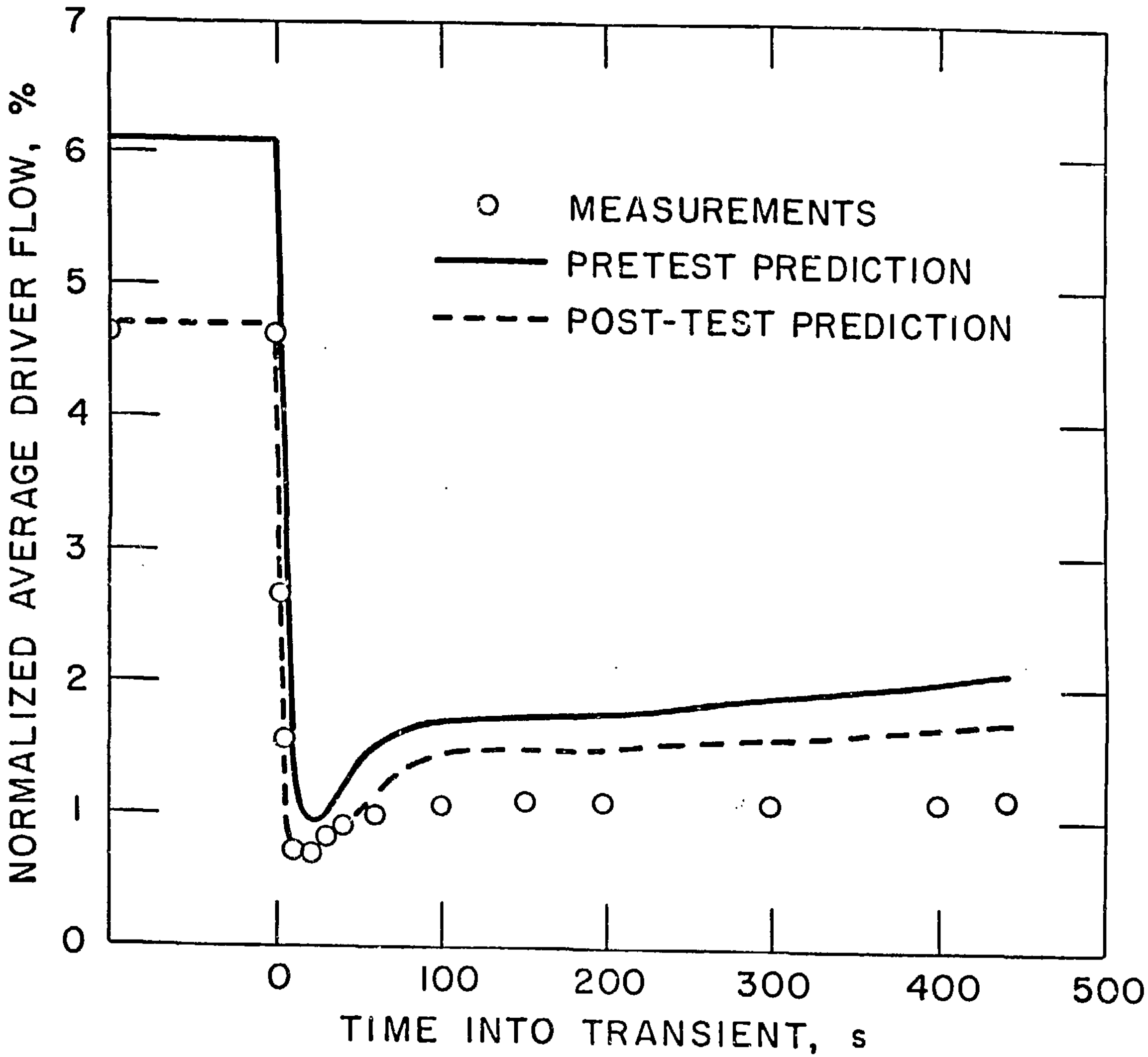

Figure 4. XX09 Flow Response During SHRT 2 Transient

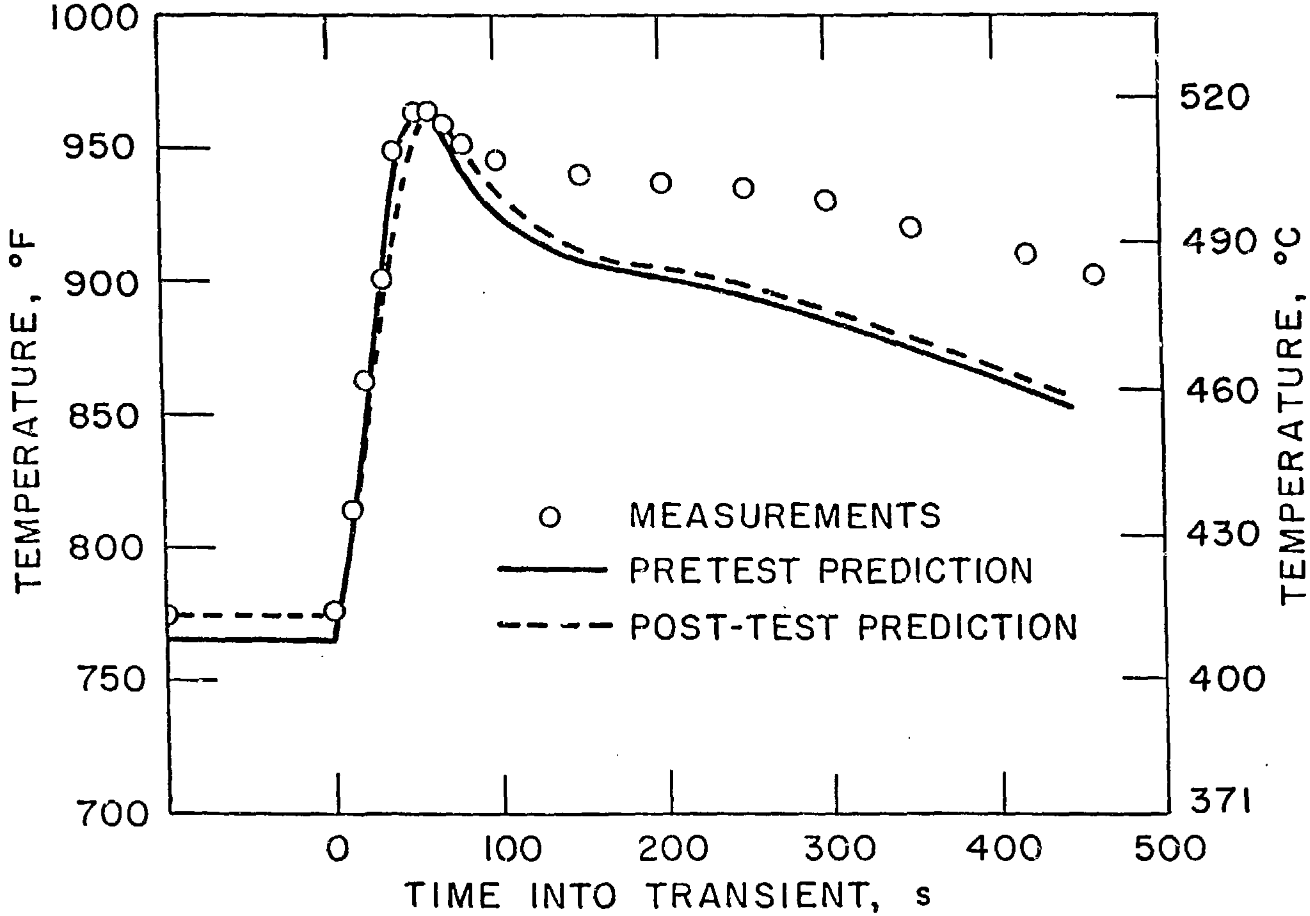

Figure 5. XX09 Temperatures at Inner Region of the TCC Location During SHRT 2 Transient

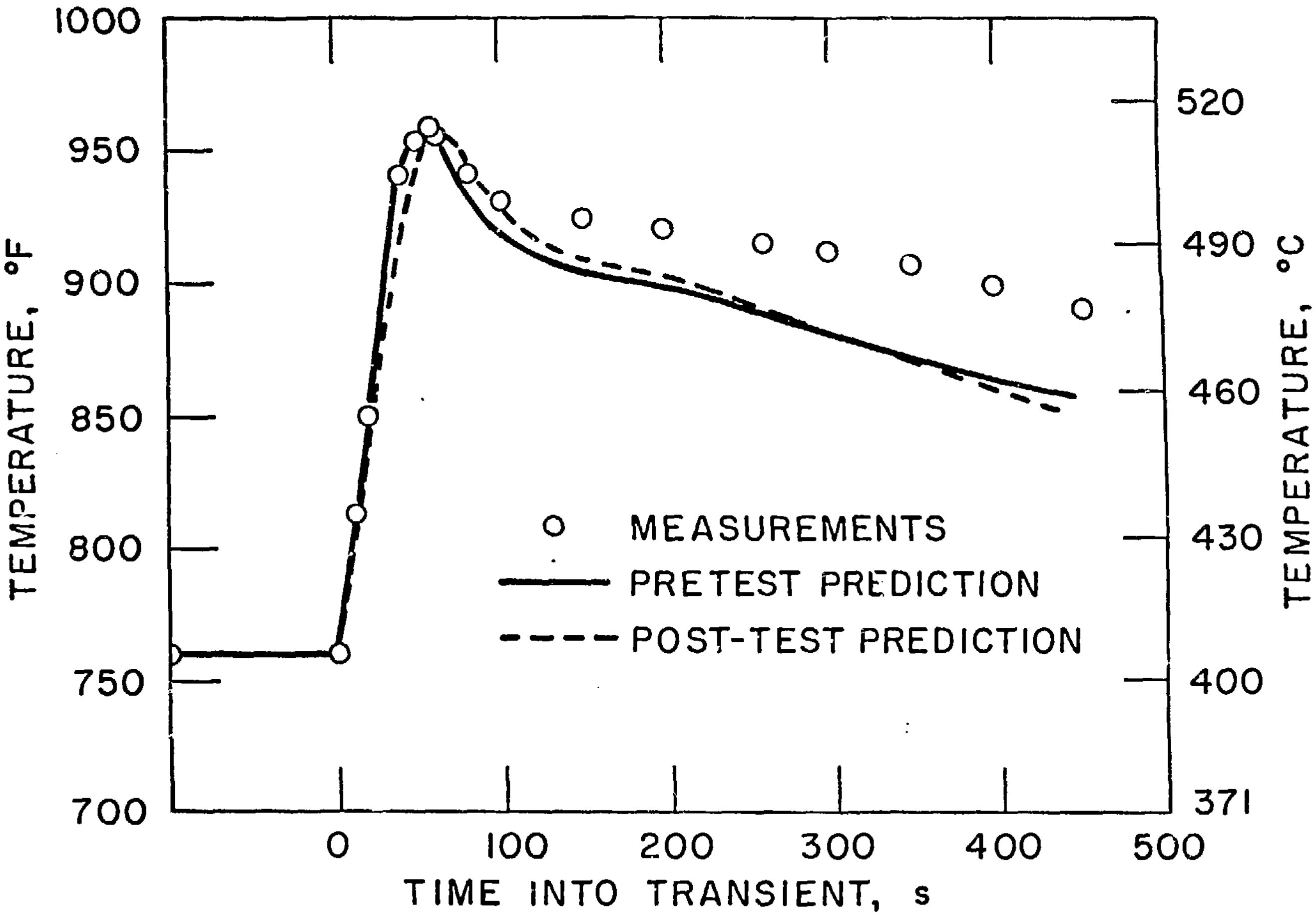

Figure 6. XX09 Temperatures at Outer Region of the TTC Location During SHRT 2 Transient

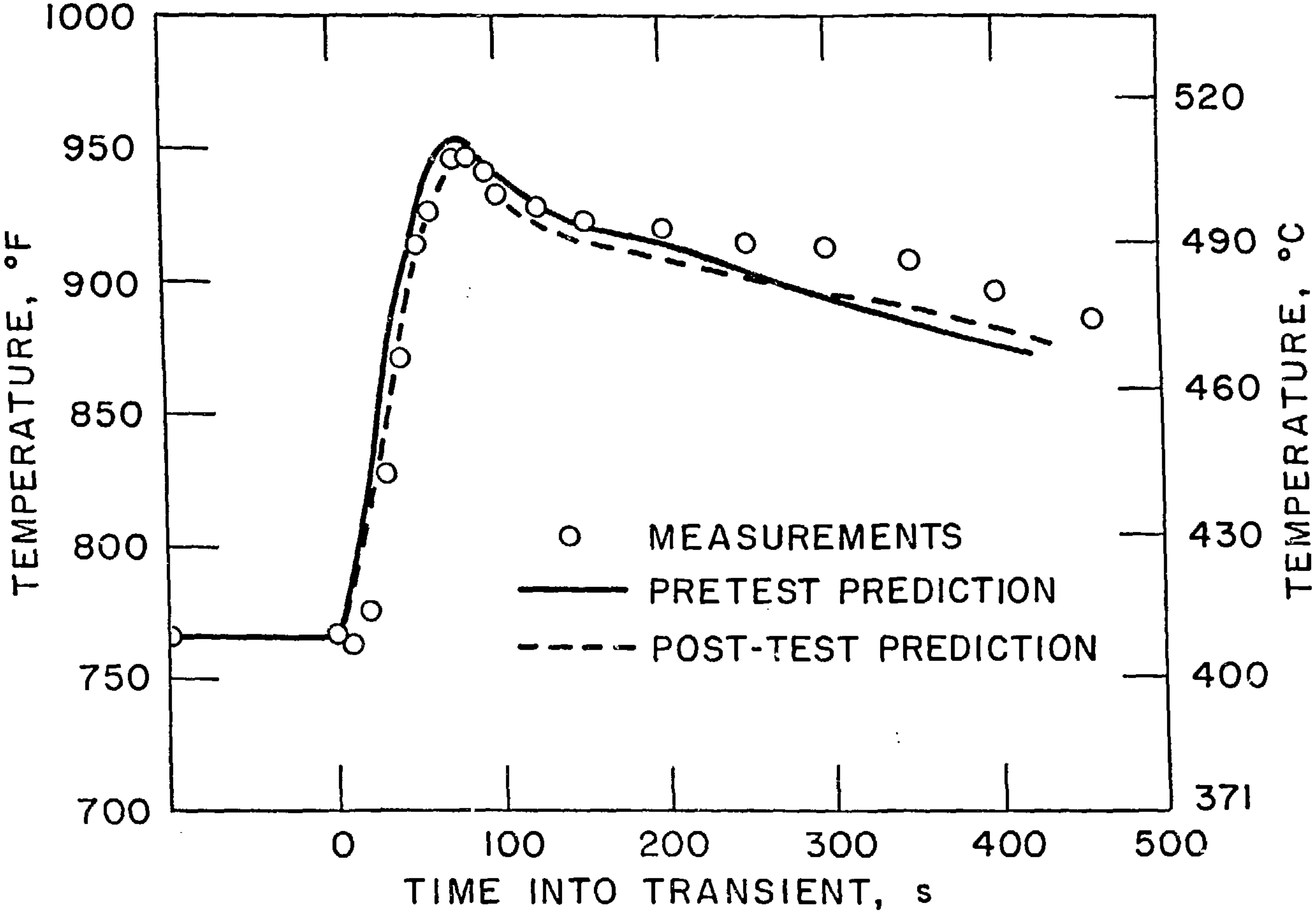

Figure 7. XX09 Temperature at 14TC Location During SHRT 2 Transient

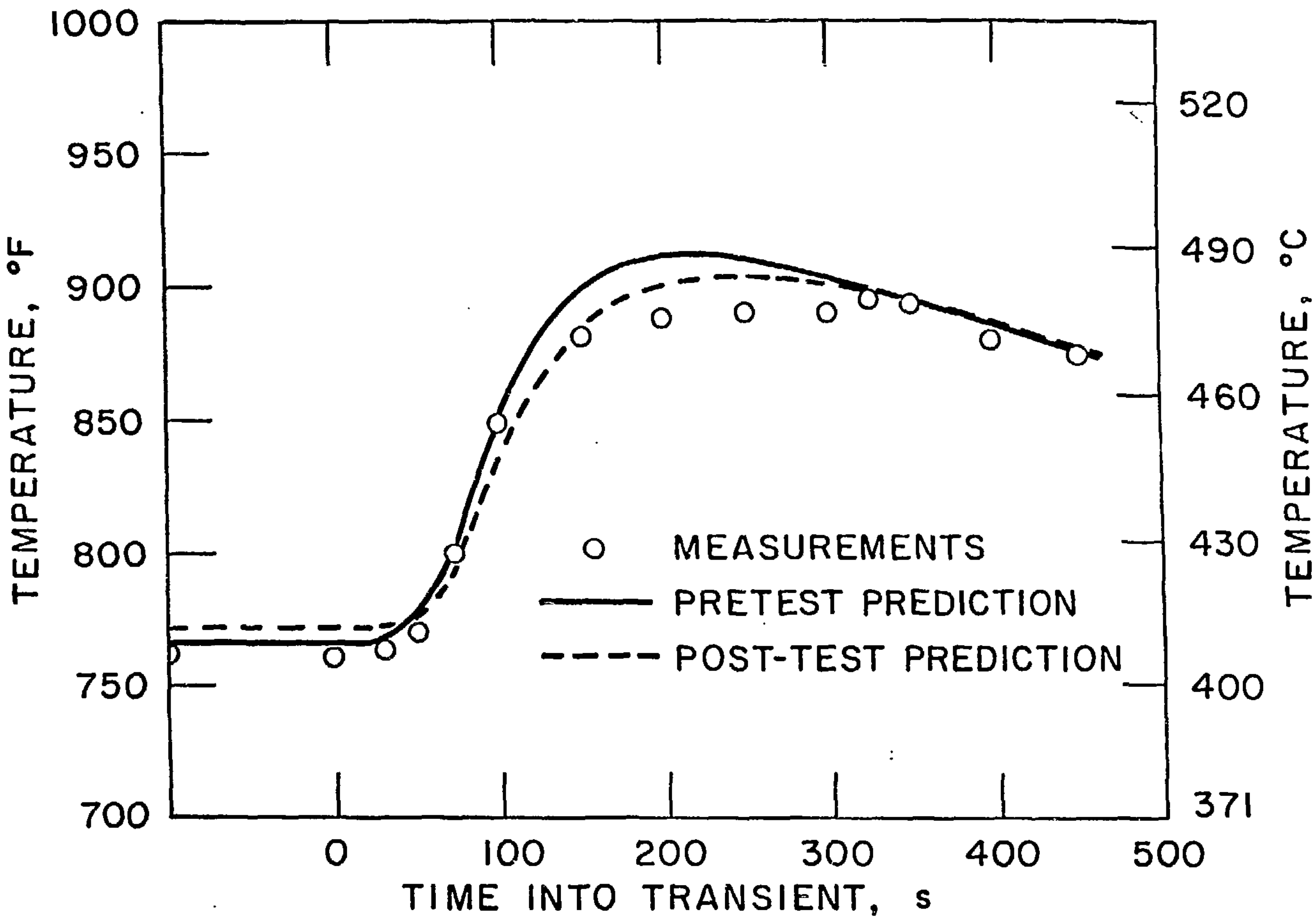

Figure 8. XX09 Subassembly Outlet Temperature During SHRT 2 Transient

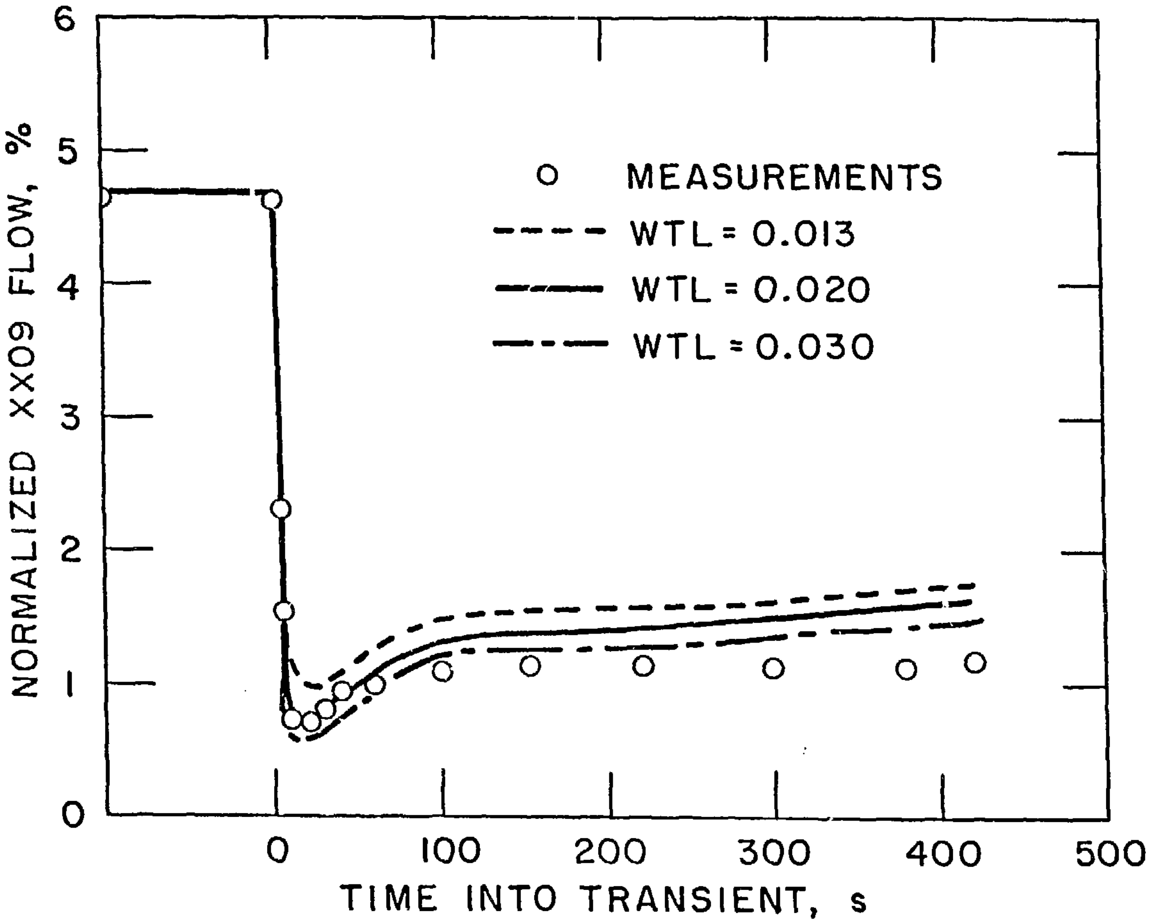

Figure 9. Effects of Turbulent-Laminar Transition on XX09 Flow During SHRT 2 Transient

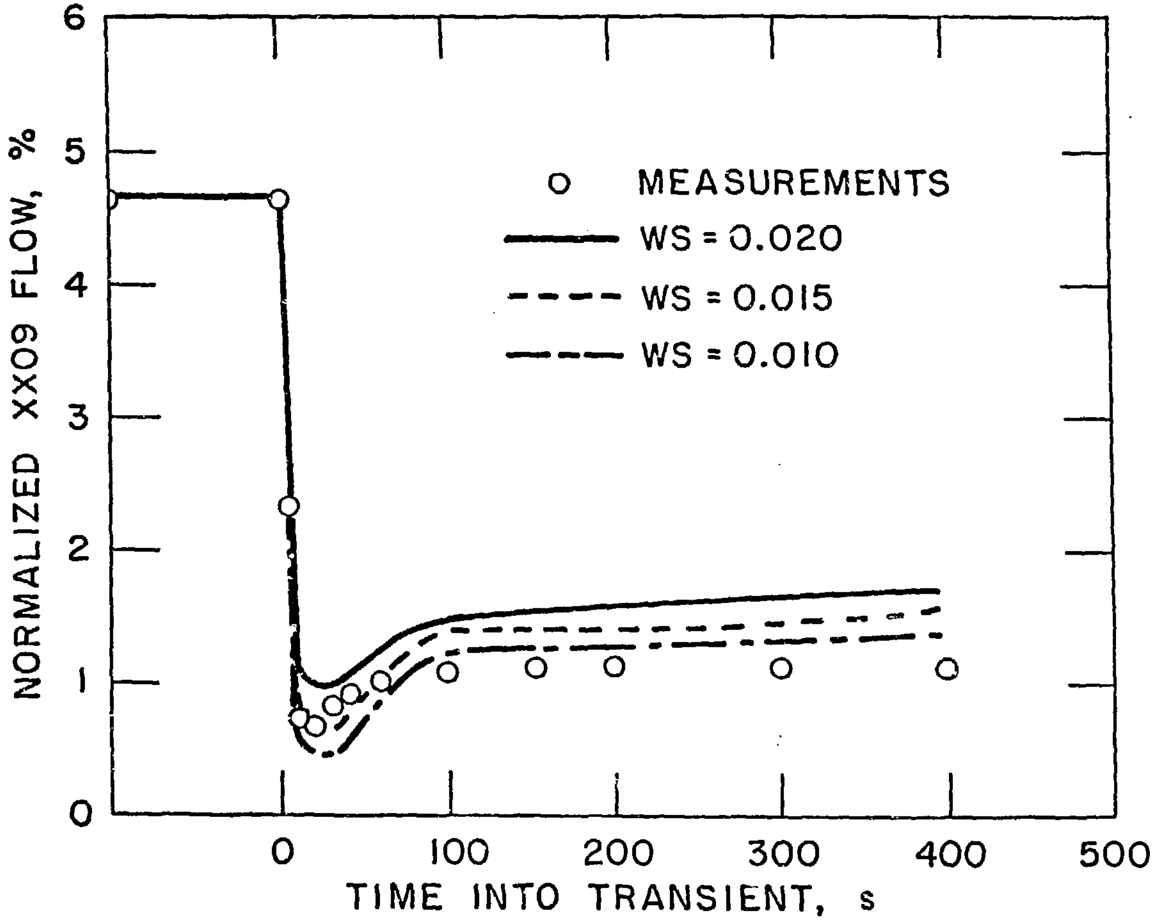

Figure 10. Effect of Secondary Flow on XX09 Flow During SHRT 2 Transient.